ON THE DESIGN OF

ZERO REACTION MANIPULATORS

Evangelos Papadopoulos
Assistant Professor, Member ASME
Department of Mechanical Engineering and
Centre for Intelligent Machines
McGill University
Montreal, PQ H3A 2A7, Canada

Ahmed Abu-Abed
Electrical Distribution and Control Division
General Electric Canada
Mississauga, ON L5N 5P9, Canada

February 12, 1996

Accepted for Publication as a Full Paper
ASME Journal of Mechanical Design

Abstract

In a number of industrial, space, or mobile applications, reaction forces and moments transmitted by a manipulator to its base are undesirable. In this paper, we analyze the problem of force and torque transmission in robotic systems, and propose design and planning methods that can eliminate it, or reduce it. Based on force and moment transmission analysis, a three DOF redundant manipulator design is selected. Dynamic reaction *forces* are eliminated by force balancing. Reaction *moments* are eliminated by following reactionless paths, whose planning is simplified by rendering the dynamics configuration-invariant. Reactionless Workspaces are defined in which any end-effector path can result in zero dynamic reactions. An example is used to demonstrate the usefulness of the proposed methods. An important advantage of these methods is that the manipulator can be used either as a redundant, or as a reduced DOF reactionless system.

1 Introduction

Reaction forces transmitted by a manipulator to its base are highly undesirable. In an industrial setting, the accuracy of a rapidly accelerating manipulator will be degraded by vibrations caused by the transmission of large reaction forces to its mounts, (Karidis et al., 1992). In space, dynamic reactions due to an accelerating manipulator mounted on a satellite will disturb the position and orientation of the latter (Dubowsky and Torres, 1991). If allowed to transmit reaction forces, manipulators operating in a micro-gravity environment will have adverse effects on it (Rohn et al., 1988). Manipulators mounted on compliant mobile bases, be it a truck, a Mars rover, or the Shuttle Canadarm, will inevitably excite the base dynamics and result in poor dynamic performance and accuracy (Erb, 1990, West et al., 1990).

Moving a manipulator slowly is the simplest way to reduce reactions to acceptable levels. However, this is not acceptable in high performance applications. Reducing manipulator reactions by cost function minimization applied to redundant manipulators was proposed (Quinn et al., 1988). Complete shaking force elimination can be achieved by adding counterweights or by relocating the support point of the manipulator (Berkof et al., 1977, Walker and Oldham, 1978).

Minimization of the rocking moment was accomplished by using an additional actuator with a preset inertia, along with a suitable controller (Karidis et al., 1992). However, such actuators can not contribute to system manipulative capabilities. In space, there exist paths that, if followed by a manipulator mounted on a free-floating spacecraft, zero attitude disturbance for the spacecraft will result (Papadopoulos, 1992). Use of such paths may require relocating the spacecraft to a favorable initial position, while reaction forces are not eliminated, i.e. the spacecraft will translate.

In this paper we analyze the transmission of force and moment reactions in manipulators and propose guidelines that can result in reactionless motions. These include force balancing of the manipulator, invariance of its mass matrix, and use of special joint-space reactionless trajectories. The concept is demonstrated with a three Degree-of-Freedom (DOF) nine link redundant manipulator with its three direct drive actuators base-mounted and sharing a common axis; with this design, reaction moments can be canceled if the actuators rotate in opposite directions. The system Center of Mass (CM) is fixed by force balancing, and the dynamics of the system are rendered invariant. The latter feature simplifies planning of reactionless paths, since they simply belong to fixed orientation joint space planes. Reactionless Workspaces are defined in which it is possible to follow any end-effector path and still eliminate dynamic forces and moments. An advantage of the proposed method is that a manipulator can be used either as a redundant or as a reduced DOF reactionless system.

2 Base Force and Moment Balancing

Consider a manipulator as a mechanism that transmits a force $\mathbf{f}_B$ and a moment $\boldsymbol{n}_B$ to its base at a single point B, see Fig. 1. A force balance for the manipulator in the presence of gravity, results in

$$\mathbf{f}_B = -\frac{d}{dt}\{M\dot{\mathbf{r}}_{CM}\} + M\mathbf{g} \tag{1}$$

where M is the total manipulator mass, $\mathbf{g}$ is the acceleration of gravity vector, and $\dot{\mathbf{r}}_{CM}$ is the velocity of the system CM. It can be seen that $\mathbf{f}_B$ has an undesired dynamic component resulting from changes in system's linear momentum, and a static component due to gravity (zero in space). The

dynamic components in Eq. (1) are zero if the system CM does not accelerate, or equivalently, if $\ddot{\mathbf{r}}_{CM}$ = const. Assuming zero initial CM velocity, integration of this condition yields $\mathbf{r}_{CM}$ = const., i.e. to transmit zero dynamic forces, the manipulator's CM has to be fixed. In principle, this condition can be achieved by design. To this end, note that by definition

$$\mathbf{r}_{CM} = \frac{1}{M}\sum_{j=1}^{l} m_j \mathbf{r}_{c,j} \tag{2}$$

where l is the number of manipulator links, m_j the mass of the jth link and $\mathbf{r}_{c,j}$ the position vector of the jth CM with respect to base frame origin B, see Fig. 1. Differentiation of Eq. (2) yields

$$\ddot{\mathbf{r}}_{CM} = \frac{1}{M}\sum_{i=1}^{n}\sum_{j=1}^{l} m_j \frac{\partial \mathbf{r}_{c,j}}{\partial q_i}\ddot{q}_i = \frac{1}{M}\sum_{i=1}^{n} \boldsymbol{\gamma}_i \ddot{q}_i = \frac{1}{M}\boldsymbol{\gamma}\ddot{\mathbf{q}} \tag{3}$$

where n is the number of DOF, $\ddot{q}_i$ is the ith joint rate, $\ddot{\mathbf{q}}$ is the $n \times 1$ vector of joint rates, and $\boldsymbol{\gamma}$ is a $3\times n$ matrix with $\boldsymbol{\gamma}_i$ its columns. Eq. (3) shows that the condition $\mathbf{r}_{CM}$ = const. can hold for *any* set of $\ddot{\mathbf{q}}$ if and only if all $\boldsymbol{\gamma}_i$ are identically equal to zero, or equivalently if $\boldsymbol{\gamma} \equiv \mathbf{0}$. In principle, the condition $\boldsymbol{\gamma}_i$ = 0 can be satisfied by proper design, usually by static balancing. However, balancing may not possible for any manipulator. For example, for planar systems without axisymmetric link groupings, force balancing by internal mass redistribution is possible if, and only if, for each link there is a path to the ground by way of revolutes only (Berkof et al., 1977). As a consequence, a planar mechanism with revolute joints can be balanced always. Therefore, in this paper we consider manipulators planar with revolute joints, only.

It is worth noting that the dynamics of a manipulator can be written as (Abu-Abed, 1993)

$$\boldsymbol{\tau} = \mathbf{H}(\mathbf{q})\,\ddot{\mathbf{q}} + \mathbf{V}(\mathbf{q},\dot{\mathbf{q}}) + \boldsymbol{\gamma}^{\mathrm{T}}(\mathbf{q})\,\mathbf{g} \tag{4}$$

where $\mathbf{H}(\mathbf{q})$ is the $n\times n$ manipulator mass matrix, $\mathbf{q} = [q_1,\ldots,q_n]^{\mathrm{T}}$ is the vector of generalized coordinates, $\boldsymbol{\tau} = [\tau_1,\ldots,\tau_n]^{\mathrm{T}}$ the vector of actuator torques, and $\mathbf{V}(\mathbf{q},\dot{\mathbf{q}})$ the vector of velocity terms. Eq. (4) shows that force balancing the manipulator, also eliminates static actuator requirements and simplifies a system's dynamics.

To study reaction moments, a moment balance written about point B in Fig. 1 yields

$$\mathbf{n}_B = \mathbf{r}_{CM} \times M\mathbf{g} - \frac{d}{dt}\left\{\sum_{j=1}^{l}\left(\mathbf{I}_j \bullet \boldsymbol{\omega}_j + m_j \mathbf{r}_{c,j} \times \dot{\mathbf{r}}_{c,j}\right)\right\} \tag{5}$$

where $\mathbf{n}_B$ is the moment transmitted to the base, $\mathbf{I}_j$ is the j[th] link inertia, and $\boldsymbol{\omega}_j$ its inertial angular velocity. The sum in Eq. (5) represents the angular momentum of the manipulator with respect to the base frame origin B, and can be equivalently written as (Papadopoulos and Dubowsky, 1991)

$$\sum_{j=1}^{l}\left(\mathbf{I}_j \bullet \boldsymbol{\omega}_j + m_j \mathbf{r}_{c,j} \times \dot{\mathbf{r}}_{c,j}\right) = \mathbf{D}(\mathbf{q})\dot{\mathbf{q}} \tag{6}$$

where $\mathbf{D}(\mathbf{q})$ is an inertia-type matrix of size $3\times n$. The static moment represented by the cross product in Eq. (5) can be eliminated by locating the system CM at point B.

Eliminating $\mathbf{n}_B$ can be achieved by using additional base actuators, such as reaction wheels, that can cancel reaction moments. This method was employed in the design of a high-acceleration minipositioner (Karidis et al., 1992), and can been used in space (Dubowsky and Torres, 1991). A limitation of this method is that any additional actuators cannot be used to increase the DOFs of a manipulator. Here, we are interested in eliminating dynamic moments using a manipulator's own design. In such case, all links and actuators can contribute to manipulation tasks.

Assuming zero initial velocities, Eqs. (5) and (6) suggest that to eliminate dynamic moments the angular momentum must be zero. However, unlike with linear momentum, in general it is not possible to set $\mathbf{D}(\mathbf{q}) = \mathbf{0}$ by design. This is because the elements of $\mathbf{D}(\mathbf{q})$ contain sums of inertia and other configuration dependent terms that cannot be set equal to zero for *all* configurations $\mathbf{q}$. Another possibility is to set $\mathbf{D}(\mathbf{q})\dot{\mathbf{q}} = \mathbf{0}$, which requires that $\dot{\mathbf{q}}$ trajectories are in the null space of $\mathbf{D}(\mathbf{q})$. This solution results in velocity constraints that reduce the available DOF of the manipulator, and therefore, redundant systems must be employed if the end-effector is to follow any desired paths in space. However, $\mathbf{D}(\mathbf{q})\dot{\mathbf{q}} = \mathbf{0}$ represents a Pfafian equation which, in general, cannot be integrated to yield constraints in terms of the joint angles $\mathbf{q}$. The nonintegrability of the angular momentum introduces nonholonomic characteristics, i.e., a closed path in joint or Cartesian space will result in a drift in a manipulator's configuration. Such features are undesirable, since after some time, some joint will reach its limits, and motion will stop. To avoid nonholonomic problems,

one can make $\mathbf{D}(\mathbf{q})$ invariant by design or, equivalently, equal to a constant matrix. Then $\mathbf{D}(\mathbf{q})\ddot{\mathbf{q}} = \mathbf{0}$ can be integrated to yield configuration constraints. This is the approach taken here.

3 Planar Manipulator Designs for Reactionless Motions

Consider a planar manipulator with revolute joints for which the dynamic reaction forces were eliminated, i.e. $\boldsymbol{\gamma} = \mathbf{0}$. Due to Eq. (4), actuator torques necessary to cancel static gravity torques are also zero. Therefore, at static conditions, $\mathbf{n}_B$ is also zero. Direct observation of Eq. (5) under static conditions shows that in such case $\mathbf{r}_{CM}$ is zero, i.e. force balancing results in zero *static* moments about the attachment point of the manipulator to its base, point B in Fig. 1.

As discussed above, a desired step in eliminating *dynamic* moments transmitted to the base is to make $\mathbf{D}(\mathbf{q})$ constant. The actual form of $\mathbf{D}(\mathbf{q})$ will depend on the mechanical design of the manipulator. If only one actuator is located at the base, then $\mathbf{n}_B$ will be necessarily nonzero, and equal in magnitude to τ_1. In such case, it will not be possible to have $\mathbf{D}(\mathbf{q})\ddot{\mathbf{q}} = \mathbf{0}$. However, if two or more actuators are mounted at the base and act along the same axis $\mathbf{k}$ containing the origin B, then it is possible to eliminate $\mathbf{n}_B$ by having torques from one actuator cancel torques of the others. Such design will certainly allow for $\mathbf{D}(\mathbf{q})\ddot{\mathbf{q}} = \mathbf{0}$, and possibly for a constant $\mathbf{D}(\mathbf{q})$. It can be shown that invariance of $\mathbf{D}(\mathbf{q})$ requires invariance of the mass matrix $\mathbf{H}$ as the elements of $\mathbf{D}(\mathbf{q})$ are linear combinations of those of $\mathbf{H}$.

From the above analysis, the following design guidelines emerge for reactionless planar manipulators: (a) force balance a manipulator with revolute joints to eliminate dynamic forces, and (b) use mass matrix invariance and special planning techniques to eliminate reaction moments. As explained above, guideline (b) introduces a constraint between the joint angles, and consequently redundant manipulator designs must be employed.

Based on this analysis, a 3 DOF nine link parallel manipulator with three actuators mounted at its base is selected that can meet the requirements for reaction-free motion. For other designs that can result in reactionless motions, see (Abu-Abed and Papadopoulos, 1994). To maintain planar operation, the manipulator is assumed to be symmetric with respect to its plane of action. As evident

from Fig. 2, this manipulator is redundant in terms of the in plane positioning requirements, and was proposed as a mechanical hand finger (Youcef-Toumi and Yahiaoui, 1988). This manipulator is composed of three parallel mechanisms; links 1-4-6 are always mutually parallel, and so are 2-5-8 and 3-7-9. Note also that the following sets of links share common lengths: $l_1 = l_4 = l_6$, $l_5 = l_8$, and $l_3 = l_7$. Each set of parallel links can be made to rotate while the other links are either stationary or translating. The driving links (1, 2, & 3) and their direct drive actuators are on the base; this simplifies decoupling of the manipulator's mass matrix and results in simpler dynamic equations. In the next section we focus on force and moment balancing this nine-link parallel manipulator.

4 Manipulator Design

To force balance the manipulator shown in Fig. 2, first the $\boldsymbol{\gamma}_i$ vectors are found according to Eq. (3), and given in Eq. (A1). Setting these equal to zero results in

$$\begin{aligned} &m_1 l_{c1} + m_4 l_{c4} + m_6 l_{c6} + (m_5 + m_7 + m_8 + m_9) l_1 = 0 \\ &m_2 l_{c2} + m_4 l_2 - m_5 l_{c5} - m_8 l_{c8} - m_9 l_5 = 0 \\ &m_3 l_{c3} + m_6 l_3 + m_7 l_{c7} + m_8 l_3 - m_9 l_{c9} = 0 \end{aligned} \tag{7}$$

where l_{ci} (i = 1,…,9) are the locations of the nine CMs, defined as shown in Fig. 2.

To obtain a reactionless constraint in terms of the joint angles **q**, the **D** matrix given in Eq. (A3) must be made invariant. This yields three more equations to be satisfied by design

$$\begin{aligned} &m_4 l_2 l_{c4} - m_5 l_1 l_{c5} - m_8 l_1 l_{c8} - m_9 l_1 l_5 = 0 \\ &m_6 l_3 l_{c6} + m_7 l_1 l_{c7} + m_8 l_1 l_7 - m_9 l_1 l_{c9} = 0 \\ &m_9 l_5 l_{c9} - m_8 l_7 l_{c8} = 0 \end{aligned} \tag{8}$$

Note that both Eqs. (7) and (8) are not functions of link inertias. Therefore, lengths l_{ci} can be adjusted by the use of constant mass counterweights. To solve for the nine l_{ci} lengths, the six equations (7) and (8) are written in compact matrix form as

$$\mathbf{A}\boldsymbol{l}_c = \boldsymbol{k} \tag{9}$$

where $\mathbf{A}$ is a 6×9 matrix and $\boldsymbol{k}$ a 6×1 vector, both functions of link masses and lengths, and $\boldsymbol{l}_c$ is a 9×1 vector that contains the unknown l_{ci}. This linear system is under-constrained and has an infinite number of solutions including the minimum-norm one. Depending on the relative importance of the l_{ci}, one can minimize $\mathbf{W}\boldsymbol{l}_c$ instead of $\boldsymbol{l}_c$, where $\mathbf{W}$ is a diagonal weighting matrix. In such case, the weighted minimum norm solution for $\boldsymbol{l}_c$ is given by

$$\boxed{\boldsymbol{l}_c = \mathbf{W}^{-1}(\mathbf{W}^{-1})^T\mathbf{A}^{\mathbf{T}}(\mathbf{A}\mathbf{W}^{-1}(\mathbf{W}^{-1})^T\mathbf{A}^{\mathbf{T}})^{-1}\boldsymbol{k}} \tag{10}$$

Using $\mathbf{W}$ = *diag* (1.0, 0.2, 1.0, 1.2, 1.0, 1.0, 1.0, 1.2, 1.0), Eq. (9) is solved and the resulting manipulator parameters are displayed in Table I.

Table I. Manipulator Parameters

i	l_i (m)	m_i (kg)	I_i (kgm^2)	l_{ci} (m)
1	0.50	7.00	0.2501	-0.2214
2	0.18	1.45	0.0025	-0.1111
3	0.20	2.00	0.0180	-0.1605
4	0.50	1.50	0.0199	0.2016
5	0.46	0.70	0.0215	-0.0110
6	0.50	1.50	0.0419	-0.0349
7	0.20	1.15	0.0143	-0.0682
8	0.46	0.50	0.0162	0.0032
9	0.30	0.25	0.0058	0.0027

It is worth pointing out that in this case, the manipulator's mass matrix is both invariant and decoupled, resulting in the following equations of motion

$$\begin{bmatrix}\tau_1\\ \tau_2\\ \tau_3\end{bmatrix} = \begin{bmatrix}h_{11} & 0 & 0\\ 0 & h_{22} & 0\\ 0 & 0 & h_{33}\end{bmatrix}\begin{bmatrix}\ddot{q}_1\\ \ddot{q}_2\\ \ddot{q}_3\end{bmatrix} \tag{11}$$

However in general, reactionless manipulators do not necessarily have a decoupled mass matrix.

5 Reactionless Path Planning

As discussed in Section 2, elimination of reaction moments requires that the angular momentum given by Eq. (6) be maintained equal to zero. For the force balanced and invariant mass matrix manipulator of the previous section, this equation is written as

$$\dot{q}_1 + \lambda_2 \dot{q}_2 + \lambda_3 \dot{q}_3 = 0 \tag{12}$$

where $\lambda_2 = h_{22}/h_{11} = d_2/d_1$, and $\lambda_3 = h_{33}/h_{11} = d_3/d_1$. This equation suggests that reactionless motions require that at least one joint be moving opposite to some other one. Since λ_2 and λ_3 are constants, Eq. (12) can be integrated to yield

$$q_1 + \lambda_2 q_2 + \lambda_3 q_3 = b \tag{13}$$

where the constant b is called the *pose constant*, and depends on the initial configuration **q**. Equation (13) represents a joint space *plane*, with $\boldsymbol{\lambda} = [1, \lambda_2, \lambda_3]^T$ its normal vector. For a reactionless motion, all via points and the target point must be on the plane defined by the b of the initial configuration **q**. Since a redundant manipulator can reach points in its workspace in more than one poses, it follows from Eq. (13) that a single x-y point can have a range of b constants associated with it. Each of these b constants defines a different plane, but since the normal vector $\boldsymbol{\lambda}$ is fixed for a given manipulator, all these planes are parallel (Papadopoulos and Abu-Abed, 1994).

Given an end-effector location in x-y space, the range of pose constants which correspond to it can be found using inverse kinematic relationships. To each of these constants corresponds a set of $q_1 - q_2 - q_3$ angles. A plot of q_1 versus the available pose constants b is shown in Fig. 3, for two (x, y) points. This plot can be used to determine if two (x, y) points can be joined by a reactionless path. To this end, a pose constant which is available to both points, or equivalently, a plot overlap should exist, such as the one in Fig. 3. For example, point (0.50, 0.50) is reachable from (0.55, 0.90), if the initial angle q_1 is between 1.6 and 1.9 rad.

Path planning can be facilitated if the set of points that can be accessed with reactionless paths from some initial configuration is known. The set of such points defines the *Reactionless Workspace* associated with a particular initial configuration. To find this workspace, it is assumed that the first joint can rotate freely, while relative joint angles $a_1 = q_2 - q_1$ and $a_2 = q_3 - q_2 + \pi$ vary within their limits. The forward kinematic equations for this manipulator are, see Fig. 2

$$x = l_1 \cos(q_1) - l_5 \cos(q_2) - l_9 \cos(q_3) \tag{14a}$$

$$y = l_1 \sin(q_1) - l_5 \sin(q_2) - l_9 \sin(q_3) \tag{14b}$$

Solving Eq. (13) for q_1 yields

$$q_1 = \frac{b}{1+\lambda_2+\lambda_3} + \frac{\lambda_3(\pi - a_2) - a_1(\lambda_2+\lambda_3)}{1+\lambda_2+\lambda_3} = b^* + \phi(a_1, a_2) \quad (15)$$

where $b^* = b/(1+\lambda_2+\lambda_3)$ is a constant, and ϕ an angle function of a_1 and a_2. Substituting Eq. (15) into Eq. (14) and using the relative joint angles a_i, Eq. (14) is written as

$$\begin{bmatrix} x \\ y \end{bmatrix} = \begin{bmatrix} c(b^*) & -s(b^*) \\ s(b^*) & c(b^*) \end{bmatrix} \begin{bmatrix} c(\phi) & -s(\phi) \\ s(\phi) & c(\phi) \end{bmatrix} \begin{bmatrix} l_1 - l_5 c(a_1) + l_9 c(a_1+a_2) \\ -l_5 s(a_1) + l_9 s(a_1+a_2) \end{bmatrix} \quad (16)$$

where c(), s() denote the cosine and the sine of an angle. For a given initial pose, b and therefore b^* are fixed. Hence, the Reactionless Workspace can be found by varying the a_i in their range. Note that since b^* only appears in the rotation matrix in Eq. (16), the *shape* of the reactionless workspace is independent of this constant. However, its *orientation* in space depends on it.

Using Eq. (16), the Reactionless Workspace is plotted in the Cartesian plane for b = 2.4 rad and depicted in Fig. 4. Any two points in this region can be connected with *any* path, to result in a reactionless motion as long as the motion in the joint space adheres to its reactionless plane. If the desired path cannot be contained in this shaded region, reaction moments will be transmitted to the base when the end-effector crosses the boundary of the reactionless workspace. Fig. 4 also depict the Reactionless Workspace corresponding to b = 5.0 rad. As expected, its shape is identical to that for b = 2.4 rad, but its orientation is different.

6 Simulation Results and Comparisons

The base reactions of the manipulator whose parameters appear in Table I were computed using its equations of motion. As expected, these parameters result in zero *dynamic force* transmission, irrespective of the path followed. To calculate reaction *moments*, initial and final points A and B were chosen from a Reactionless Workspace as follows: (x_A, y_A) = (0.50, 0.50) and (x_B, y_B) = (0.55, 0.90), with corresponding b = 2.4 rad. To test the effect of different paths on the base reactions moments, the following three paths were chosen

1. A path planned in Cartesian space, independent of any reactionless requirements.
2. A path planned in the configuration space; the path did not adhere to any reactionless plane.
3. A reactionless path. In Cartesian space, the path was identical to that in Case 2 above. The x-y pairs along with the *b* constant determine the initial and final angles of the manipulator, $\mathbf{q}_A$ and $\mathbf{q}_B$, see Eqs. (13) and (14). The path was a straight line in joint space connecting $\mathbf{q}_A$ and $\mathbf{q}_B$, both lying on the plane defined by Eq. (13).

Quintic polynomial trajectories were used in the simulation to result in continuous joint velocity and acceleration profiles. A computed torque control scheme was employed to determine motor torques, while the control gains were the same in all three cases. The required actuator torques τ_1, τ_2, and τ_3, as well as the resultant base reaction are shown in Fig. 5. Snapshots of the corresponding motion sequences of links 1, 5 and 9 are also shown. As depicted in Figs. 5 (a) and (b), the resulting reaction moment is high for Cases 1 and 2, since no reactionless plane is adhered to. For Case 3, Fig. 5 (c) shows that throughout the motion the base reaction moment is zero.

Although the above analysis indicates zero base reactions, small deviations from the ideal zero reaction case may occur in practice. Sources of such deviations include manufacturing tolerances, neglected small unbalanced friction in the direct drive actuators, and manipulator unbalance due to a payload. However, in all these cases the proposed design will eliminate the most significant base reactions which are due to manipulator accelerating links. Finally, note that in principle higher DOF spatial reactionless manipulators can be constructed using as building blocks two or three DOF reactionless manipulators. On the other hand, since most of the base reactions are due to the proximal links of a manipulator, one can use the proposed methods to reduce such reactions significantly.

7 Conclusions

Analysis of force transmission properties of manipulators has shown that dynamic reactions can be eliminated if the system Center of Mass is kept fixed. For planar mechanisms with revolute joints, this condition can be satisfied by proper design. However, elimination of reaction moments requires in general appropriate trajectory planning. Rendering a system's mass matrix invariant, simplifies

the planning of reactionless paths, since they only need to be on fixed orientation joint space planes. A three-DOF planar manipulators was designed based on analysis, and was used to demonstrate the value of the proposed methods. An advantage of this design is that the manipulator can be used either as redundant, or as reduced DOF reactionless system.

Acknowledgments

Support by the Fonds pour la Formation de Chercheurs et l'Aide a la Recherche, and by the Natural Sciences and Engineering Council of Canada is gratefully acknowledged.

References

Abu-Abed, A. and Papadopoulos, E., 1994, "On the Design of Zero Reaction Robots," *Proc. of the CSME Forum*, Montreal, Canada.

Abu-Abed, A., 1993, "Analysis and Design of Planar Zero Reaction Robots," McGill Centre for Intelligent Machines Internal Report CIM 93-24, Montreal, Canada.

Berkof, R.S., et al., 1977, "Balancing of Linkages," *Shock and Vibration Digest., Vol*. 9, No. 6, pp. 3-10.

Dubowsky, S. and Torres, M.A., 1991, "Path Planning for Space Manipulators to Minimize Spacecraft Attitude Disturbance," *Proc. 1991 IEEE Conf. on Robotics and Automation*, Sacramento, CA.

Erb, B., 1990, "Canada's Mobile Servicing System," *Space Technology*, Vol. 10, No 1/2, pp. 19-25.

Karidis, J.P., et al., 1992, "The Hummingbird Minipositioner - Providing Three Axis Motion at 50 G's With Low Reactions," *Proc. 1992 IEEE Conf. on Robotics and Automation*, Nice, France.

Papadopoulos, E. and Abu-Abed, A., 1994, "Design and Motion Planning for a Zero-Reaction Manipulator," *Proc. of the IEEE Int. Conf. on Robotics and Automation*, San Diego, CA, pp. 1554-1559.

Papadopoulos, E. and Dubowsky, S., 1991, "On the Nature of Control Algorithms for Free-floating Space Manipulators," *IEEE Trans. on Robotics and Automation*, Vol. 7, No. 6, pp. 750-758.

Papadopoulos, E., 1992, "Path Planning for Space Manipulators Exhibiting Nonholonomic Behavior," *Proc. of the Int. Conf. on Intelligent Robots and Systems (IROS '92)*, Raleigh, NC, pp. 669-675.

Quinn, R.D., et al., 1988, "Redundant Manipulators for Momentum Compensation in a Micro-Gravity Environment," *AIAA Guidance, Navigation, and Control Conf.*, Minneapolis, MN, August 15-17.

Rohn, D., et al., 1988, "Microgravity Robotics Technology Program," *ISA/88 Int. Conf.*, Houston, TX.

Walker, M.J. and Oldham, K., 1978, "General Theory of Force Balancing Using Counterweights," *Mechanism and Machine Theory*, 13, pp. 175-185.

West, H., et al., 1990, "Experimental Simulation of Manipulator Base Compliance," *in Experimental Robotics I*, V. Hayward, and O. Khatib (Eds.), Lect. Notes in Control and Information Sciences #139, Springer Verlag.

Youcef-Toumi, K. and Yahiaoui, M., 1988, "The Design of a Mini Direct-Drive Finger With Decoupled Dynamics," *ASME 1988 Winter Annual Meeting*, pp. 411-415.

Appendix A

For the 3 DOF manipulator in Fig. 2, the columns of the $\boldsymbol{\gamma}$ matrix in Eq. (3) are

$$\boldsymbol{\gamma}_1 = \boldsymbol{\alpha}_1[m_1 l_{c1} + m_4 l_{c4} + m_6 l_{c6} + (m_5 + m_7 + m_8 + m_9) l_1]$$

$$\boldsymbol{\gamma}_2 = \boldsymbol{\alpha}_2[m_2 l_{c2} + m_4 l_2 - m_5 l_{c5} - m_8 l_{c8} - m_9 l_5]$$

$$\boldsymbol{\gamma}_3 = \boldsymbol{\alpha}_3[m_3 l_{c3} + m_6 l_3 + m_7 l_{c7} + m_8 l_3 - m_9 l_{c9}] \qquad \text{(A1)}$$

where $\boldsymbol{\alpha}_k$, (k = 1,2,3), are given by

$$\boldsymbol{\alpha}_k = \begin{bmatrix} -\sin(q_k) & \cos(q_k) & 0 \end{bmatrix}^T \qquad \text{(A2)}$$

The elements of matrix $\mathbf{D}(\mathbf{q}) = [d_1, d_2, d_3]$ are given by

$$
\begin{aligned}
d_1 &= I_1 + I_4 + I_6 + m_1 l_{c1}^2 + m_4 l_{c4}^2 + m_6 l_{c6}^2 + (m_5 + m_7 + m_8 + m_9) l_1^2 + \\
&+ (m_4 l_2 l_{c4} - m_5 l_1 l_{c5} - m_8 l_1 l_{c8} - m_9 l_1 l_5) \cos(q_1 - q_2) + \\
&+ (m_6 l_3 l_{c6} + m_7 l_1 l_{c7} + m_8 l_1 l_7 - m_9 l_1 l_{c9}) \cos(q_1 - q_3) \\
d_2 &= I_2 + I_5 + I_8 + m_2 l_{c2}^2 + m_5 l_{c5}^2 + m_8 l_{c8}^2 + m_4 l_2^2 + m_9 l_5^2 + \\
&+ (m_4 l_2 l_{c4} - m_5 l_1 l_{c5} - m_8 l_1 l_{c8} - m_9 l_1 l_5) \cos(q_1 - q_2) \\
&+ (m_9 l_5 l_{c9} - m_8 l_7 l_{c8}) \cos(q_2 - q_3) \\
d_3 &= I_3 + I_7 + I_9 + m_3 l_{c3}^2 + m_7 l_{c7}^2 + m_9 l_{c9}^2 + m_6 l_3^2 + m_8 l_7^2 + \\
&+ (m_6 l_3 l_{c6} + m_7 l_1 l_{c7} + m_8 l_1 l_7 - m_9 l_1 l_{c9}) \cos(q_1 - q_3) \\
&+ (m_9 l_5 l_{c9} - m_8 l_7 l_{c8}) \cos(q_2 - q_3)
\end{aligned}
\qquad \text{(A3)}
$$

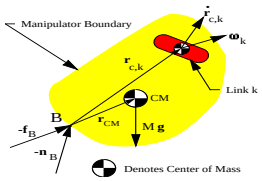

Fig. 1. Forces and moments applied on a manipulator.

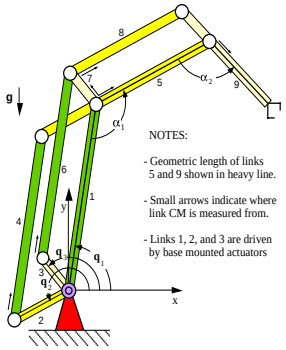

Fig. 2. A nine-link 3 DOF parallel manipulator.

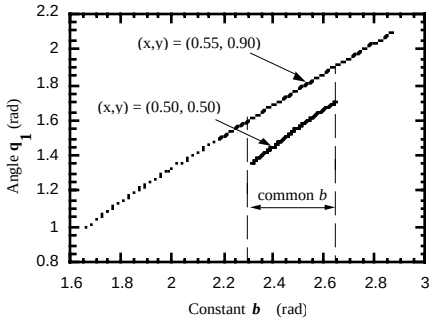

Fig. 3. Range of q_1 and corresponding *b* pose constants for two (x, y) points

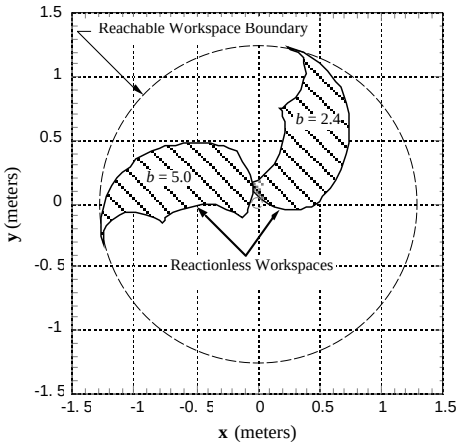

Fig. 4. Reactionless workspaces for b = 2.4 rad, and b = 5.0 rad.

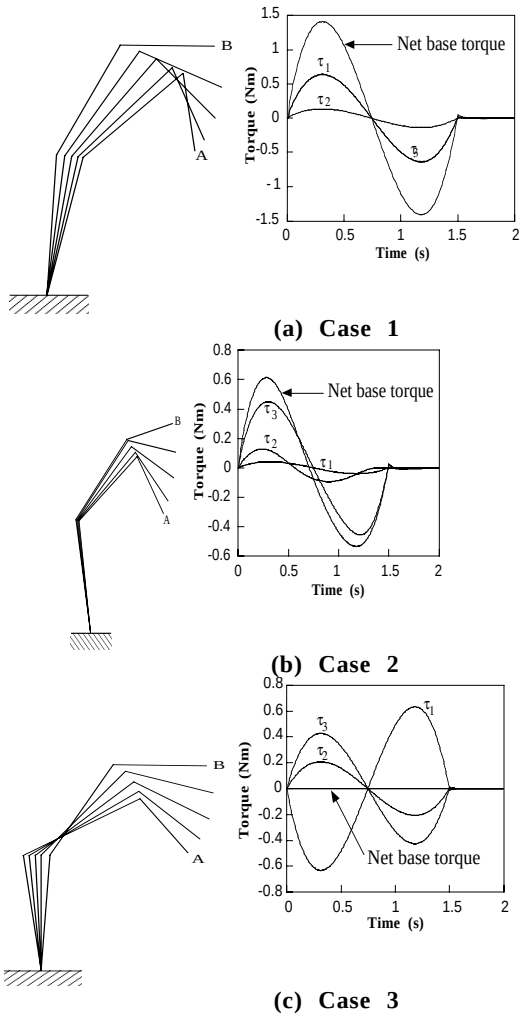

Fig. 5. Manipulator snapshots and corresponding torque profiles. End-effector paths start at point A, and end at point B. (a) Path planned in Cartesian space, (b) Path planned in joint space, (c) Reactionless path.